Antibacterial activity of therapeutic agent-immobilized nanostructured TiCaPCON films against antibiotic-sensitive and antibiotic-resistant *Escherichia coli* strains

Elizaveta S. Permyakova[a,*], Philipp V. Kiryukhantsev-Korneev[a], Viktor A. Ponomarev[a], Alexander N. Sheveyko[a], Sergey A. Dobrynin[b], Josef Polčak[c], Pavel V. Slukin[d], Sergey G. Ignatov[d], Anton Manakhov[a], Sergei A. Kulinich[e,f], Dmitry V. Shtansky[a,*]

[a]*National University of Science and Technology "MISIS", Leninsky prospect 4, Moscow, 119049, Russia*

[b]*N.N. Vorozhtsov Novosibirsk Institute of Organic Chemistry of the Siberian Branch, Russian Academy of Sciences, Novosibirsk, Russian Federation*

[c]*CEITEC - Central European Institute of Technology, Brno University of Technology, Purkyňova 123, Brno, Czech Republic*

[d]*State Research Center Applied Microbiology and Biotechnology, Russia, Moscow, Russian Federation*

[e]*Research Institute of Science and Technology, Tokai University, Hiratsuka, Kanagawa 259-1292, Japan*

[f]*Department of Mechanical Engineering, Tokai University, Hiratsuka, Kanagawa 259-1292, Japan*

* Correspondence: permyakova.elizaveta@gmail.com (E.S.P.); shtansky@shs.misis.ru (D.V.S.)

Tel.: +7-916-278-0199 (E.S.P.); +7-499-236-6629 (D.V.S.)

ABSTRACT

The development of flexible and low-cost methods of surface functionalization to fight infection at the early stage is an urgent scientific task. Herein, polymerization in low-pressure plasma rich in COOH species and carbodiimide chemistry methods were utilized to immobilize four different therapeutic agents (antibiotic (gentamicin), antimicrobial peptide (indolicidin), anti-adhesive molecules (heparin) and nitroxide radicals (2,2,5,5-tetramethyl-3- carboxyl-pyrrolidine-1-oxyl)) on the surface of nanostructured biocompatible TiCaPCON films to impart antibacterial characteristics. The polymers deposited from COOH-rich plasma showed decent stability in phosphate-buffered saline solution and were successfully used for the immobilization of different therapeutic agents *via* ionic or covalent bond. The bactericide attachment was proved by FTIR spectroscopy and XPS analysis. All samples with grafted therapeutic agents were hydrophilic with water contact angle values in the range of 26-56°. Bactericide release tests indicated the maximum concentration of therapeutic agents in the case of ionic immobilization. In case of covalent immobilization, fast initial release observed over 24 h was followed by slower leaching in the next 24 h (indolicidin), 48 h (heparin), and 96 h (gentamicin). The pH-sensitive COOH plasma polymer degradation and gentamicin release were demonstrated. The bactericide-linked films showed noticeable reduction of the antibiotic-sensitive *E. coli* U20 strain and, except indolicidin-immobilized samples, effectively inhibited growth of the antibiotic-resistant *E. coli* K261 strain at their initial concentration of 10^4 CFU/mL. The films with nitroxide radicals not only exhibited the highest antibacterial activity against *E. coli* K261 cells (100% after 8 h), but also prevented the biofilm formation.

1. Introduction

Bacterial infection is one of the main causes of implant failure. Most bacteria do not exist in free-floating form and tend to form biofilm [1]. A biofilm is a combination of bacteria (5-35%) and a specific environment that attaches to the surface and increases the physical and chemical resistance of bacteria as much as 100-1000 times [1-3]. An effective way to avoid implant-related infections is to inhibit biofilm formation by creating antibacterial surface.

One of the promising approaches aimed at creating antibacterial materials is the immobilization of a therapeutic agent on their surfaces [4]. In case of highly porous materials, a widely used method is to soak them in an antibiotic solution. However, physical adsorption is known to result in fast bactericide release [5,6]. Recent developments showed that coated implant with a biodegradable polymer can inhibit fast release of therapeutic agent, permitting to control the content of bioactive molecules and minimizing both local and entire toxicity associated with a high concentration of antimicrobial compound [2,7]. For example, the degradation rate of biodegradable polymethacrylic anhydride (PMAH) coating loaded with rifampicin obtained *via* a mild vapor polymerization process (iCVD) [8] was highly pH-sensitive (15 times faster at pH 10 compared with pH 1). The hydrolysis rate of atmospheric plasma deposited polymers obtained in the process of poly(ε -caprolactone) monoacrylate (PCLMA) polymerization was also pH-dependent [9]. After 14 days of incubation of ppPCLDA thin films in a phosphate buffer solution (PBS) at $37^{o}C$ and pH 7, their thickness was halved and after their treatment in a more alkaline environment at elevated temperature (pH 12, 95 ^{o}C) a full degradation within 5 days was observed. The antibiotic release rate from ampicillin-loaded β-tricalcium phosphate (β-TCP) materials coated with PEG-like films deposited by low pressure radio-frequency plasma polymerization of diglyme was 10 times lower compared with their untreated counterparts [10]. Several studies demonstrated the promise of plasma polymers with –COOH or -NH$_2$ functional groups in immobilization of different therapeutic agents such as antibiotics [11,12], anti-adhesive molecules [13,14], antimicrobial peptides (AMPs) [15] and other bactericides [14,15].

Using different surface functionalization approaches and immobilization mechanisms, the formation of relatively stable antibiotic/film conjugates on metal [16] and polymer [17] surfaces is possible, which prevents a rapid dissolution of bactericidal components and ensures long-term antibacterial protection. Compared to conventional antibiotics, AMPs have several advantages, such as original amphipathic nature and immunomodulatory ability [18]. Indolicidin is the shortest antimicrobial peptide (13 amino acids) that has high antibacterial activity against Gram-positive and Gram-negative bacteria [19]. When selecting anticoagulant therapeutic agent, its cost, availability of antidotes, route of administration, safety and efficacy are important factors to be considered.

Heparin, a sulfated polysaccharide, is the most common clinical anticoagulant [20] which is also globally used for the creation of antibacterial coatings [21].

Recently there has been an increased interest in reactive oxygen species as antibacterial agents [22,23]. In particular, NO-donor compounds were widely utilized to create antibacterial coatings [24-26]. Low concentration of nitric oxide (10^{-12}-10^{-9} M) was found to affect the biofilm, transferring bacteria to a dispersed state [27]. This effect of nitric oxide can be explained by reduction in cyclic di-GMP level, which plays a key role in biofilm formation [28]. However, since nitric oxide has extremely high chemical reactivity (its half-life being 0.1-5 s), the NO-donor molecules are often unstable. Nitroxides have the same structure (nitrogen atom linked to a univalent oxygen atom), but incorporation of NO group in heterocycle stabilizes the radical species [29]. Moreover, nitroxides are typically air-stable crystalline solids, which facilitates conducting experiments compared with gaseous nitric oxide [30].

A series of 23 nitroxides was tested to suppress *Pseudomonas aeruginosa* biofilm and mixed-culture biofilm growth [31]. The different activity of nitroxide compounds depending on the cycle and type of substituting radicals was observed. To provide decent antibacterial properties, the concentration of nitroxide compound was found to be in the 10^{-3} M range, or it should be mixed with antibiotics [32,33].

A crosslinking reaction between antibacterial component and substrate surface is very important for long-lasting bactericidal effect. The aim of this work was to study the possibility of immobilization of four different types of therapeutic agents (antibiotic (gentamicin), antimicrobial peptide (indolicidin), anti-adhesive molecules (heparin) and nitroxide radicals (2,2,5,5-tetramethyl-3- carboxyl-pyrrolidine-1-oxyl)) on the surface of nanostructured TiCaPCON film and to evaluate their antibacterial activity toward antibiotic-sensitive (U20) and antibiotic-resistant (K261) *Escherichia coli* strains. These films were chosen because of their biocompatibility previously confirmed in clinical trials of coated Ti implants [34]. In addition, various surface groups present on the TiCaPCON surface (OH, COOH, N-C=O) [16] could act as active cites for polymer grafting. Two different immobilization methods (electrostatic and covalent bond) affecting therapeutic agent adhesion strength and its release kinetics were considered. The successful grafting of bactericide agents and their stability in PBS were confirmed by thorough XPS and FTIR analysis.

2. Materials and methods

2.1. Reagents

The following reagents were used: 1-ethyl-3-(3-dimethylaminopropyl)carbodiimide (EDC), N-hydroxysulfosuccinimide (NHS), 2,2,5,5-tetramethylpyrrolidin (Sigma Aldrich), indolicidin (PepTech), gentamicin sulfate, heparin (BelMed), dimethyl sulfoxide (DMSO), disodium phosphate, potassium dihydrogenphosphate (Cupavnareactive).

2.2. Deposition of TiCaPCON films

TiCaPCON films were deposited onto the surface of rotated single-crystal $Si_{(100)}$ wafers by DC magnetron sputtering of a composite $TiC-CaO-Ti_3PO_x$ target (125 mm in diameter) produced by the self-propagating high-temperature synthesis method. Silicon substrates were fixed in the sample holder at a distance of 80 mm from the target and etched with Ar ions for 10 min prior to film deposition to get rid of surface contamination. The deposition process was carried out for 30 min in a gaseous mixture of Ar and N_2 with a nitrogen partial pressure of 15% at a current and a magnetron power of 2 A and 800 W, respectively.

2.3. Deposition of polymers from COOH-rich plasma

The deposition of polymers from COOH-rich plasma onto the surface of TiCaPCON films was carried out using a UVN-2M vacuum system evacuated to a pressure below 5×10^{-3} Pa. The capacitively coupled radio-frequency (RF) plasma was generated by a Cito1310-ACNA-N37A-FF (Comet, USA) RF power supply unit coupled with a RFPG-128 plasma generator (Beams&Plasmas, Russia). High-frequency power (500 W, 13.56 MHz) was supplied in a pulsed mode (duty cycle 5%, pulse duration 2 ms). The deposition time was 2 min to avoid delamination of the polymer layer. High purity Ar (99.9995 %), CO_2 (99.995%), and C_2H_4 (99.95%) gases (NiiKM) were used as precursors, with gas flow rates being set at 25, 90 and 25 ml/min, respectively. Pristine Si wafers (100 mm in diameter) and TiCaCOPN-coated Si substrates were placed opposite to the RF-antenna at a distance about 80 mm.

2.4. Immobilization of therapeutic agents on COOH-TiCaPCON and CO-NH$_2$-TiCaPCON surfaces

Therapeutic agents used were divided into two groups: amino-containing (gentamicin and indolicidin) and carboxy-containing (heparin and 3-carboxypyroxyl) molecules. The immobilization scheme is presented in Figure 1. To activate the carboxyl groups of plasma-generated polymers deposited on the surface TiCaPCON films, standard protocols of carbodiimide chemistry (NHS/EDC) were used [35]. The aqueous mixture of NHS (C = 5 mM) and EDC (C = 2 mM) was

added to COOH-TiCaPCON samples at pH 5.5. After incubation in the aqueous solution for 15 min, sample COONHS-TiCaPCON was washed in distilled water. Then samples COONHS-TiCaPCON and COOH-TiCaPCON were placed in 2 mL of PBS solution (pH 7.4) with amino-containing compounds (gentamicin (C = 40 mg/mL), indolizidine (C = 0.05 mg/mL) and ethylenediamine (500 times dilution of EDA, ≥99%)) for covalent immobilization and electrostatic conjugation, respectively, where they were kept for 2 h, after which were washed with distilled water and dried.
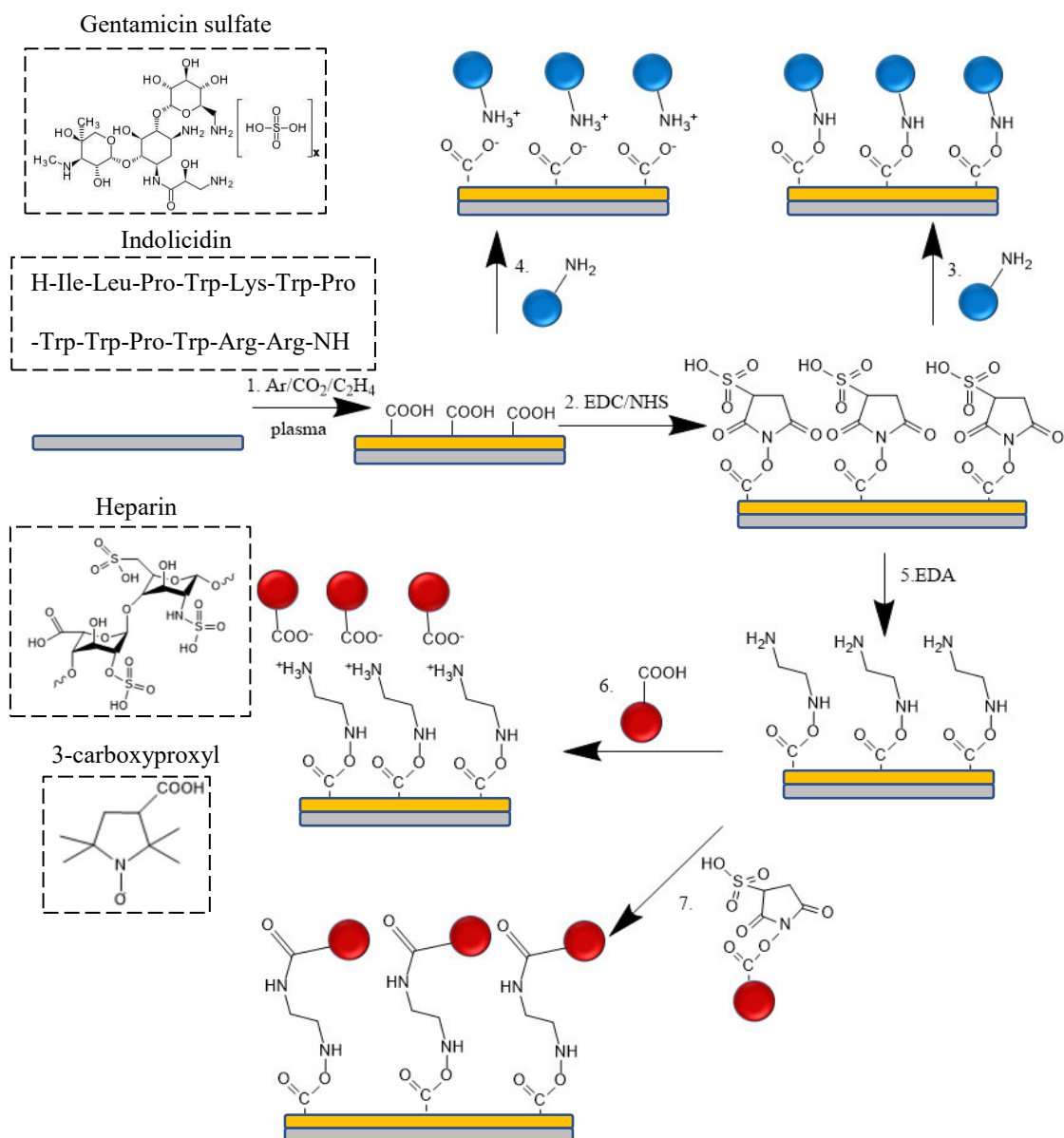
Fig. 1. Scheme of immobilization with therapeutic agents: deposition of polymer from plasma (1); immobilization of gentamicin and indolicidin by covalent (2,3) and electrostatic (4) bonds; amino-modification of plasma-produced polymer (5); heparin and 3-carboxypyroxyl conjugation by electrostatic (6) and covalent (7) bonds.

3-Carboxy-proxyl was prepared as previously described elsewhere [36]. Since 3-carboxy-proxyl did not dissolve in aqueous medium, it was initially dissolved in 100 µL of DMSO and then adjusted to the required concentration by adding water. For electrostatic attachment of heparin and nitroxide species, samples with covalently bonded EDA ($CONH_2$-TiCaPCON) were immersed in 2 mL of heparin solution (C = 5000 i.u./mL) and 3-carboxy-proxyl solution (C = 4 mg/mL), respectively, for 2 h. To immobilize heparin and 3-carboxy-proxyl by covalent bond, their respective solutions were added into an aqueous EDC/NHS mixture to activate carboxyl groups and then sample $CONH_2$-TiCaPCON was immersed in these mixtures at pH 7.4 for 2 h.

2.5 Film microstructure

The microstructure of TiCaPCON film was studied by a JEM-2100 transmission electron microscopy (JEOL Ltd.). To observe the polymer layer on the surface of TiCaPCON film and to determine the film element composition, a JSM F7600 scanning electron microscope (JEOL Ltd.) equipped with a silicon drift EDX detector X-Max 80 mm was used.

2.6. Surface characterization

The chemical composition of surfaces was analyzed by X-ray photoelectron spectroscopy (XPS) using an Axis Supra spectrometer from Kratos Analytical. The maximum lateral area analyzed was 0.7 mm. The spectra were fitted using the CasaXPS software after subtracting Shirley-type background. The binding energy (BE) values for carbon, titanium, and nitrogen species were taken from the available data [33,37,38]. The BE scale was calibrated by shifting the CH_x peak to 285.0 eV.

Infrared spectra (100 scans) were recorded with an increment of 4 cm^{-1} on a Vertex 80v Fourier-transform infrared (FTIR) spectrometer from Bruker with a parallel beam transmittance accessory. The spectra were collected at room temperature (20–25 °C). Water contact angle (WCA) measurements were carried out on an Easy Drop Kruss device from KRÜSS. Surface topography and roughness were analyzed using atomic force microscopy (AFM) on an NTEGRA Spectra II (NT-MDT Spectrum instrument, Russia) in a semi-contact mode.

2.7. Kinetics of therapeutic agent release

Samples with immobilized antibacterial substances were immersed in flasks filled with 5 mL of PBS (pH 7.4) at room temperature. To analyze bactericide concentration, 500 µL of each

supernatant was collected after 1, 3, 6, and 12 h and further after 1, 3, 5, and 7 days. After each sampling, the solution volume was increased to the initial level by adding 500 μL of fresh PBS. The antibiotic release kinetics was studied on an UV spectrophotometer (Ocean Optics). Measurements were performed in the wavelength range of 0-1000 nm. The maximum absorption intensities for gentamicin and 3-carboxy-proxyl were 224 [39] and 253 nm [40], respectively. The absorbance spectra of heparin and indolicidin have a double-peak appearance, with maxima at 222.3 and 256.4 nm for heparin and 224.0 and 277.9 nm for peptide. These data were used to plot calibration curves. The concentration of bactericidal molecules released from the sample surface into PBS over time was evaluated by comparing with a corresponding calibration curve. All experiments were carried out in triplicate for each antibacterial agent.

The pH-sensitive release was studied on the example of gentamicin-immobilized system. The antibiotic loading doze was determined by dissolving a gentamicin-bonded polymer film in *n*-hexane followed by spectrophotometric analysis. N-hexane dissolved free polymer was used as a control. The loading doze was found to be 224 μg/cm^2. Then the samples were placed in buffer solutions with pH values of 5.3, 7.4, and 9.3 (three samples for each pH). Amount of released gentamicin was determined after 4, 8, 24, 48, and 72 h.

2.8. Antibacterial tests

Antibacterial activity of the bactericide-bonded COOH-TiCaPCON samples was studied toward gram-negative *Escherichia coli* U20 (antibiotic-sensitive) and K261 (antibiotic-resistant) clinically isolated bacterial strains. Before the tests, all samples were UV sterilized from a distance of 15 cm for 60 min. The test samples were divided into three groups. The samples in the first group remained intact, whereas the others were placed in 0.5 mL of aqueous NaCl (9 g/L, normal saline solution, hereafter denoted as NSS) and incubated in a thermostat at 37 °C for 24 h (second group) and 48 h (third group). Upon the incubation, the samples were transferred to wells of a 24-well plate each filled with 0.5 mL of NSS for bactericidal analysis. Sample-free wells, as well as those with Si and bactericide-free COOH-TiCaPCON plates, were used as controls. Then, 0.03 mL of overnight bacterial culture was added to the plates with samples in NSS (bacterial concentration was 10^4 colony forming units *per* mL (CFU/mL)). Aliquots (0.04 mL) were taken after 0, 3, 8 and 24 h incubation in a thermostat at 37 °C. The concentration of CFU was determined by decimal dilution in 0.3 mL of NSS. From each dilution, 0.01 mL of bacterial suspension was spread on a Petri dish with Mueller Hinton Agar nutrient medium (HiMedia, India), dried in a closed dish at room temperature for 10 min, and cultivated in a thermostat at 37 °C for 24 h. Finally, the concentration of CFU was calculated. The pH value of bacterial suspension during antibacterial tests was 7.2.

To study the ability of bactericide-bonded COOH-TiCaPCON films to inhibit biofilm growth, the modified coupon method was used [41]. Samples (coupons) were incubated with bacteria in NSS. After 24 h, they were taken from solution, washed twice with 10 mL of sterile NSS (to wash out loosely attached planktonic bacterial cells from samples), sonicated in 5 mL of NSS at amplitude of 2 μm for 2 min (to disintegrate a formed biofilm into individual bacterial cells) for further determination of the CFU concentration. In all experiments, for each probe three measurements were performed. All data were presented as mean ± standard deviation. The statistical significance was assessed by the analysis of variations.

3. Results

3.1. Microstructure and morphology of TiCaPCON and polymer/TiCaPCON films
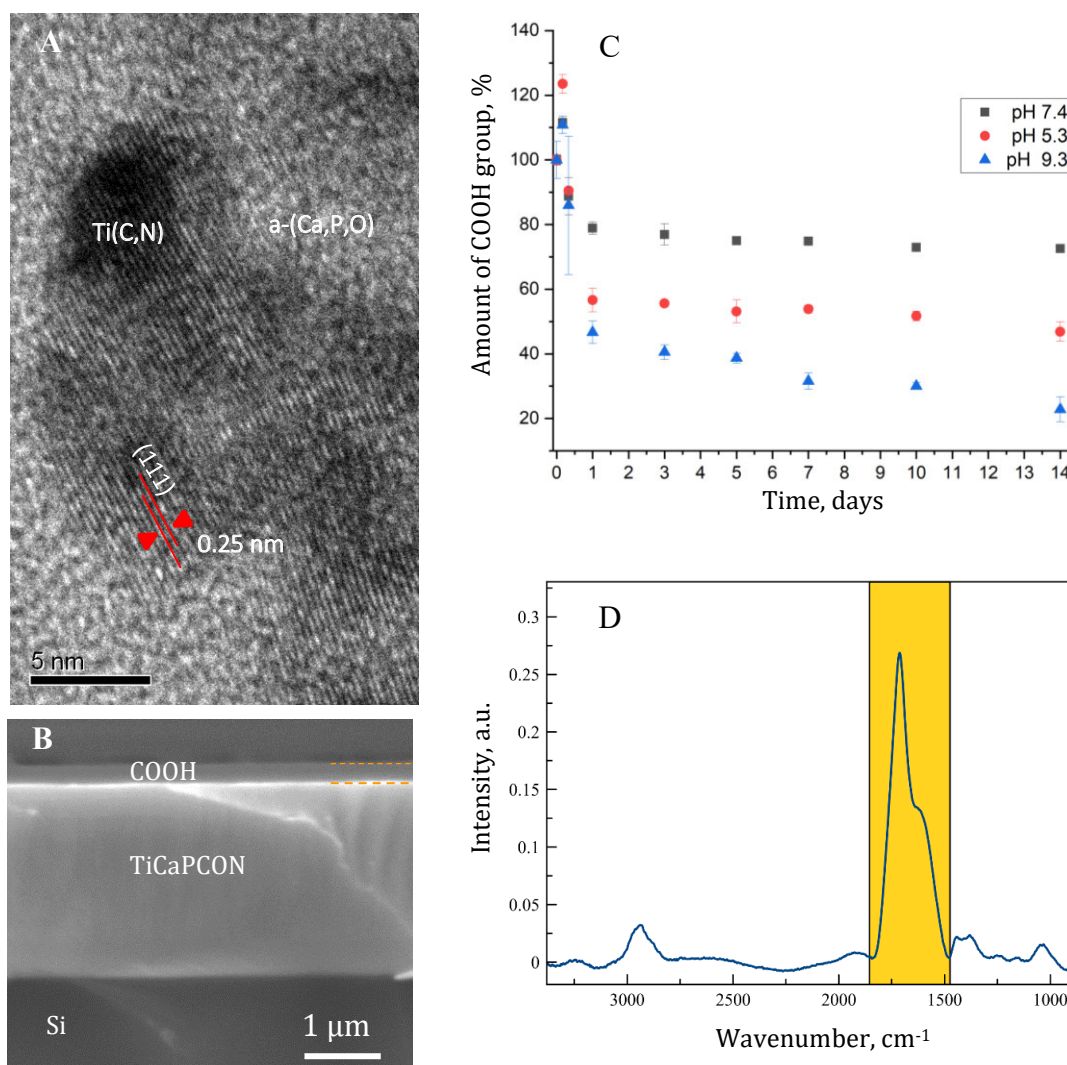
High-resolution TEM image of the TiCaPCON film is shown in Figure 2A. The film consists of Ti(C,N) crystallites, 10-15 nm in size, embedded in an amorphous matrix formed by Ca, P, and O. This nanostructuring is important to simultaneously provide high mechanical properties and accelerated osseointegration [34]. According to EDS analysis (not shown), the film contains (at.%): Ti - 43, C - 32, N - 15, O – 8, Ca – 1.5, and P – 0.5. More details about the structure of such TiCaPCON films can be found elsewhere [42].

Typical SEM micrograph of a plasma-prepared polymer coating on the surface of TiCaPCON film is shown in Figure 2B. For clear SEM visualization of the polymer layer, the deposition time was increased 10 times (from 2 to 20 min). Both the film and polymer layer are seen to have featureless morphology. The polymer layer in Figure 2B is approximately 230 nm thick and homogeneously covers the film surface.

3.2. Stability of polymers deposited from COOH-rich plasma

The stability of carboxyl groups of plasma-deposited polymers at different pH was studied by soaking sample COOH-TiCaPCON in PBS solutions with pH 5.3, 7.4, and 9.3 (Figure 2C). The amount of carboxyl groups was estimated using FTIR spectroscopy by determining the peak area (S) corresponding to ester groups which is observed in the range of 1800-1620 cm^{-1} (Figure 2D). The degree of COOH-group degradation was estimated as the S_t/S_0 ratio, where S_0 and S_t are the peak areas before and after immersion in the solution for time t, respectively. The highest degradation rate of ester/carboxyl groups was in an alkaline medium (53% after 24 h). Acidic environment also accelerated the degradation of functional groups (44% after 24 h), whereas at pH

7.4, the degree of ester/carboxyl group degradation was relatively low (~ 20% within 24 h). With further exposure to PBS environment, the dissolution rate of COOH polymer markedly decreased. In neutral medium (pH 7.4), the COOH amount was almost constant over time. In acidic medium, a slow degradation of ester/carboxyl groups was observed from 0.57 (after 1 day) to 0.47 (after 14 days). The maximum dissolution rate was in alkaline medium where the COOH amount decreased from 0.47 to 0.22. These results indicate that the pH-sensitive plasma-deposited polymers can be used as a "smart" platform for the immobilization of therapeutic agents and their controlled release in response to a change in pH.

Fig. 2. High-resolution TEM micrograph of TiCaPCON film (A). SEM micrograph showing plasma-deposited polymer on the surface of TiCaPCON film (B). Amount of COOH groups after sample COOH-TiCaPCON was exposed to PBS solutions at different pH (C). Typical XPS C1s spectrum of plasma-deposited polymer (D).

3.3. Surface topography

Surface topographical features may affect bacterial attachment and adhesion. Figure 3 illustrates surface topographies of the TiCaPCON and polymer/TiCaPCON films as determined by AFM. Without a polymer layer, the TiCaPCON surface is covered with 3D islands with an average lateral size of about 100 nm. The island height is seen to vary from 1.5 to 6.5 nm and the maximum height is approximately 10 nm. The surface roughness parameters (average roughness, R_a, and average distance between peaks, S_m) were found to be 1.18 nm and 0.11 μm, respectively. In the AFM phase mode, the island boundaries are clearly visible. To reveal the dependence of surface topography on polymer layer thickness, the deposition experiments were carried out for 2 and 20 min. In case of a thin polymer layer (deposition for 2 min) the island height was found to change within the range of 3.5-8.5 nm (R_a=1.44 nm and S_m=0.14 μm). The lateral island size remained unchanged, indicating that at the beginning of growth, the polymer layer inherited the topography of underlying TiCaPCON. Thus, the deposition of a thin polymer layer only slightly affected the average surface roughness, mainly due to the growth of polymer islands on the TiCaPCON hilltops. Further increase in deposition time to 20 min only slightly affected the average surface roughness as the island height was found to vary from 2.5 to 6.5 nm, with R_a being of 1.52 nm. However, the maximum lateral size of islands increased (S_m=0.2 μm). This observation indicates that for thicker polymer layers, their surface becomes smoother. Summing up, a change in surface roughness in the range of 1.18-1.52 nm should not have a significant effect on the bacteria adhesion.

3.4. Surface chemistry

The therapeutic agents were immobilized on the sample surfaces either by covalent bonds or *via* electrostatic interaction as shown in Figure 1. Except for the unmodified TiCaPCON film, the FTIR spectra of all samples (Figure 4) are seen to contain hydrocarbon components as evidenced by the presence of aliphatic C–H stretching vibrations in the range of 3000-2800 cm^{-1}, carboxyl/ester groups (C=O stretching at 1730 cm^{-1}), and OH band (broad peak with a maximum at ~3460 cm^{-1}). The sample with electrostatically conjugated gentamicin sulfate (panel A) reveals enhanced intensity in the range of 1500-1200 cm^{-1} with a maximum at 1280 cm^{-1} caused by sulfate (antisymmetric stretching vibrations of O-sulfate group) [12]. Moreover, the presence of OH groups from sulfate enhances intensity in the area of high wavenumbers with a maximum at ~3460 cm^{-1}. In the case of covalent gentamicin sulfate immobilization, heparin, and 3-carboxy-proxyl, the peaks at 1630 cm^{-1} that can be attributed to amide N-C=O bond are observed. The indolicidin immobilization by both types of chemical bonds (electrostatic and covalent) led to the appearance

of peak at 1630 cm^{-1} in their FTIR spectra due to the presence of -N-C=O bonds in the peptide structure (panel B).
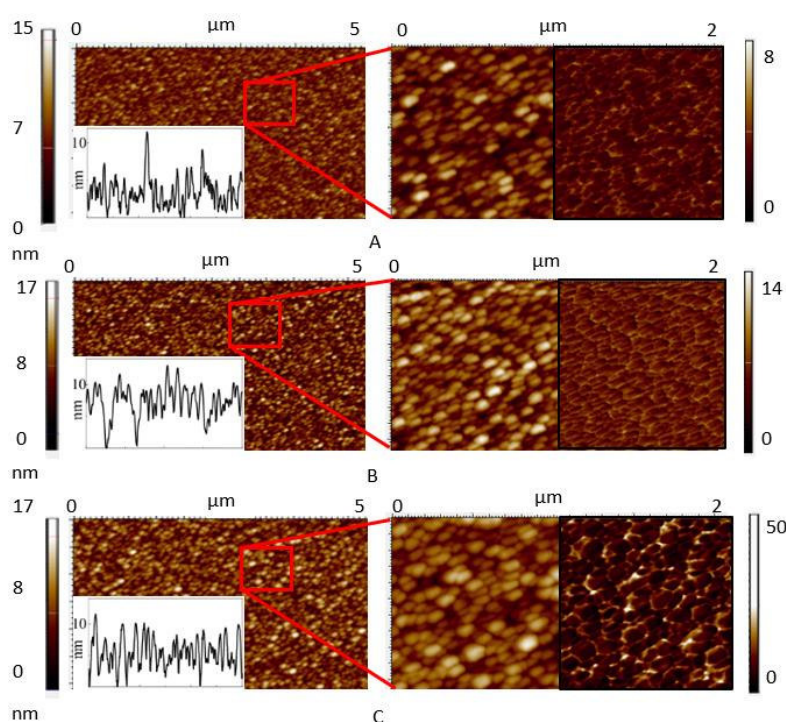
Fig. 3. AFM topographic and phase contrast (insets) images of TiCaPCON (A), TiCaPCON-polymer (2 min) (B) and TiCaPCON-polymer (10 min) films (C).

To immobilize molecules with carboxyl groups, samples COOH-TiCaPCON were initially treated by EDA. Two characteristic bands at 3415 and 3330 cm^{-1} observed in the FTIR spectrum of as-obtained sample EDA-TiCaPCON were assigned to the unsymmetrical and symmetrical -NH$_2$ stretching of primary amine. The observed broadening of peak at 1730 cm^{-1} toward lower wavenumber values could be caused by the formation of amide bond (1630 cm^{-1}) and N-H bending (1650-1580 cm^{-1}). The successful conjugation of heparin was proved by the peaks corresponding to the sulfate groups (S=O and O-H stretching). The maximum at 1550 cm^{-1} is a fingerprint of N-O stretching indicating 2-carboxy-proxyl immobilization [43].

All types of surface modifications led to a decrease in the WCA when compared with the prestine TiCaPCON film (Table 1). The WCA values decreased in the following sequence: gentamicin (49.5 – 55.8°) $\rightarrow$ peptide (37.5 – 42.5°) $\rightarrow$ heparin (33.8-38.3°) $\rightarrow$ nitroxide radicals (23.4 – 26.0°).
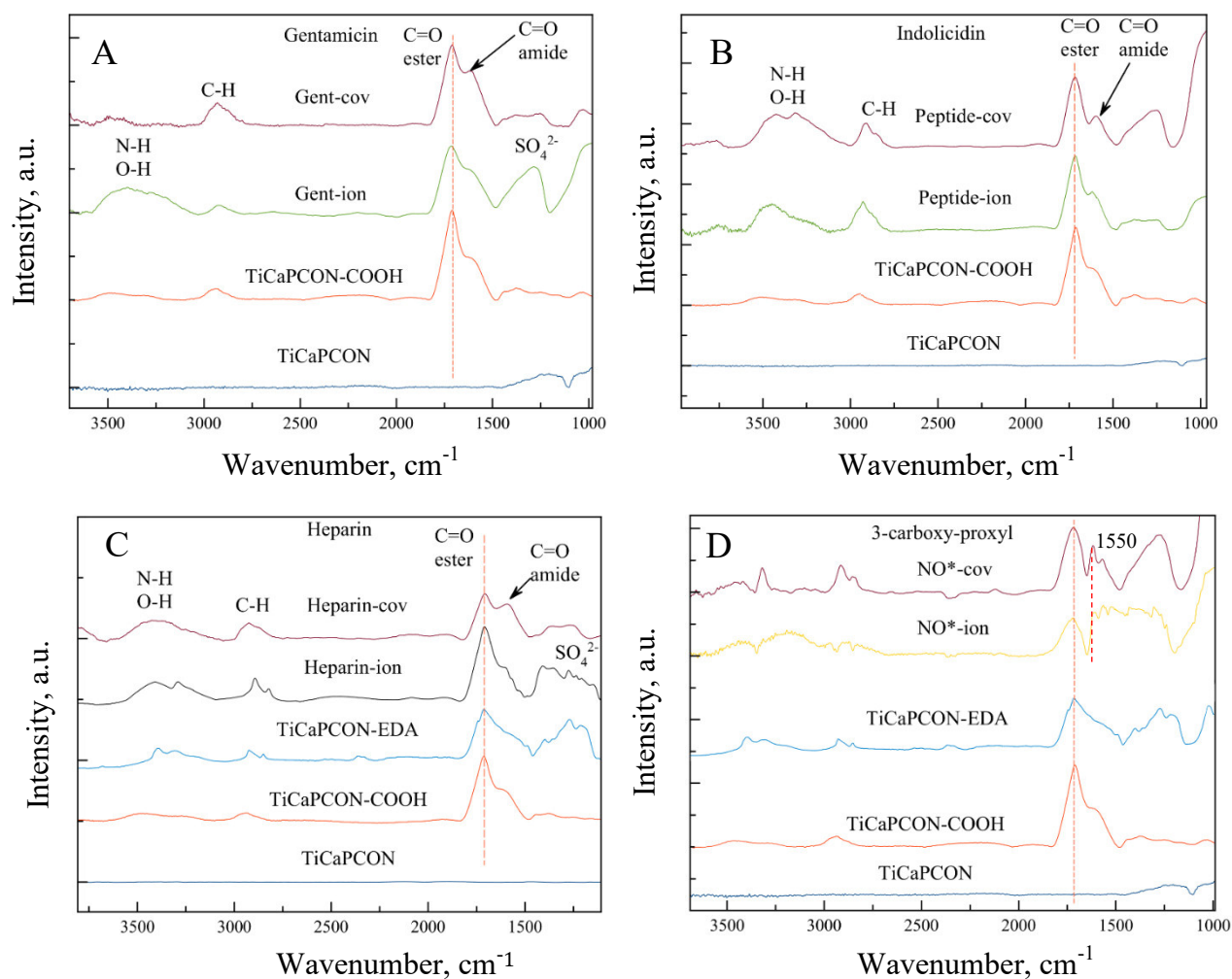
Fig. 4. FTIR spectra of gentamicin- (A), indolicidin- (B), heparin- (C) and 3-carboxy-proxyl-immobilized (D) samples.

Table 1

Water contact angles on sample surface.

Sample	WCA, º
TiCaPCON	64.0±1.9
COOH-TiCaPCON	50.6±1.1
EDA-COOH-TiCaPCON	49.6±2.3
Gent$_{COV}$-TiCaPCON	55.8±1.5
Gent$_{ION}$-TiCaPCON	49.5±2.1
Pept$_{COV}$-TiCaPCON	42.5±1.8
Pept$_{ION}$-TiCaPCON	37.5±1.2
Hepa$_{COV}$-TiCaPCON	38.3±1.7
Hepa$_{ION}$-TiCaPCON	33.8±1.4
NO$_{COV}$-TiCaPCON	23.4±1.6
NO$_{ION}$-TiCaPCON	26.0±3.2

The surfaces with immobilized theraupeutic agents were further studied by XPS. The selected XPS C1s, N1s, and O1s spectra of bactericide-congugated TiCaPCON films are presented in Figure 4 to show the most characteristic signs of each antibacterial compound. The XPS C1s spectrum of plasma-deposited polymer (Figure 5A) was fitted with a sum of four components: hydrocarbons CH_x (BE=285.0 eV, used for BE scale calibration), carbon singly-bonded to oxygen C-O (BE= 286.5 eV), carbon doubly-bonded to oxygen C=O (BE=287.8 eV), and carbon of ester or carboxylic group C(O)O (BE= 289.0 eV). The XPS analysis shows that the plasma-deposited polymer only consists of carbon and oxygen. The surface immobilization of gentamicin, indolicidin, and EDA on the surface of plasma-treated samples led to the appearance of nitrogen-associated peaks in the corresponding XPS spectra (Figure 5B-D). The XPS N1s spectra of EDA- and indolicidin-grafted samples were fitted using two components: amide group N-C=O (BE = 399.9 eV) and protonated amines NH_3^+ (BE = 401.9 eV). The XPS N1s spectrum of sample $Gent_{ION}$-TiCaPCON was fitted as a sum of three components: nitrogen-bound carbon (C-N, BE=399.1 eV), amines (NH_2, BE = 400.2 eV), and protonated amines (NH_3^+, BE = 401.9 eV). The immobilization of 3-carboxy-proxyl resulted in the formation of a new peak at 406.7 eV in the XPS N1s spectrum (Figure 5E), which was assigned to nitroxide NO component.

Taking into account the presence of sulfur in the heparin-modified sample (Table 2), its XPS O 1s spectrum was deconvoluted in several C-, H-, and S-containing components. Characteristic bands of surface C=O and C–O species are at the BE of 532.8 eV and 531.8 eV, respectively. Moreover, the deconvolution suggests the presence of three additional components at 532.9, 534.3, and 535.6 eV. The most pronounced component with a binding energy of 532.9 was assigned to oxygen in SO_4^{2-} (Figure 5F). The other two peaks of low intensity appear to belong to water molecules in the vicinity of ion. These molecules may appear on the surface of concentrated acid due to its interaction with atmospheric water and form hydrogen bonded species. Due to the presence of two protons in the molecule of sulfuric acid, the first coordination shell of these species should contain H_2O/H_3O^+ (the corresponding peak at 534.3 eV in Figure 5F). A third water molecule can serve as a bridge between neighboring "hydrates", thus forming a network that can be expressed by the general formula $[(H_3O^+) (SO_4^{2-})(H_3O^+)\cdots H_2O]_n$ (peak at 536.6 eV in Figure 5E).

The elemental compositions of sample surfaces derived from the XPS data are summarized in Table 2. It is seen that the surface composition of the samples after immobilization of amino-containing compounds is very similar and varies just within a very narrow concentration range: 71.8-75.7 (C), 3.4-6.0 (N), and 19.6-24.8 (O). The presence of sulfur (SO_4^{2-} ions) in the corresponding XPS O1s spectra confirms the conjugation with heparin by ion interaction (Figure 5F), heparin covalent immobilization, and the electrostatic grafting of gentamicin (XPS O1s spectra are not shown, Table 2). Summarizing the results of FTIR spectroscopy and XPS, it can be

concluded that all therapeutic agents have been successfully attached to the surfacte of plasma-polymerized TiCaPCON films *via* ionic or covalent bond.
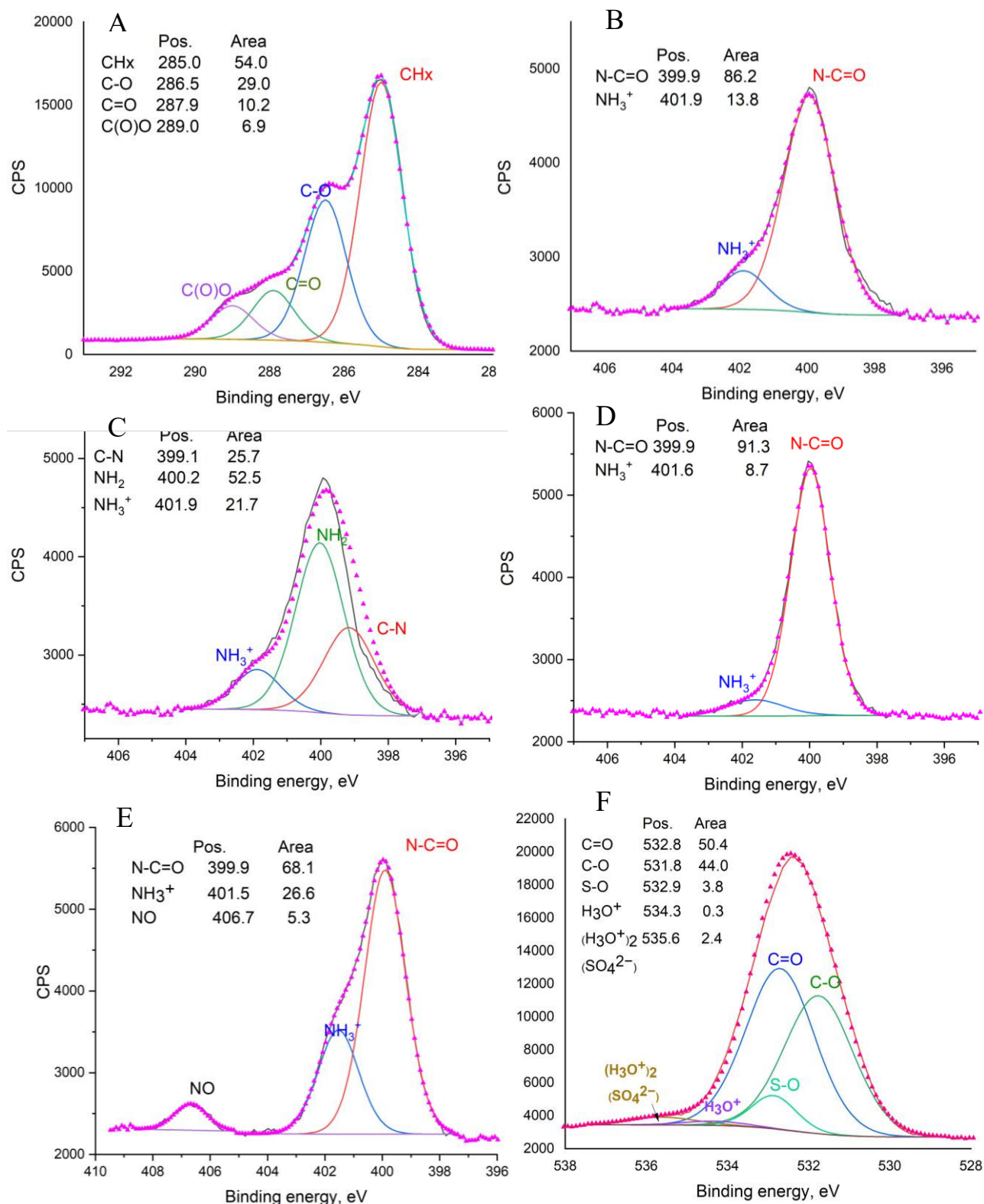
Fig. 5. XPS C1s (A), N1s (B-E), and O1s (F) spectra. Plasma-deposited polymer (A), EDA-TiCaPCON film (B), electrostatically-immobilized gentamicin (C), indolicidin (D), 3-carboxy-proxyl (E), and heparin (F).

Table 2

Atomic composition of samples derived from XPS data.

Sample	C	N	O	Ca	S
COOH-TiCaPCON	75.5	-	24.5	-	-
EDA-TiCaPCON	67.7	8.5	23.6	0.25	-
Gent$_{ION}$-TiCaPCON	75.2	5.2	19.6	-	0.2
Gent$_{COV}$-TiCaPCON	75.4	5.0	19.6	-	-
Pept$_{ION}$-TiCaPCON	75.7	4.9	19.4	-	-
Pept$_{COV}$-TiCaPCON	75.7	4.9	19.5	-	-
NO$_{ION}$-TiCaPCON	71.8	3.4	24.8	-	-
NO$_{COV}$-TiCaPCON	75.2	4.8	20.0	-	-
Hepa$_{COV}$-TiCaPCON	74.9	4.8	19.7	0.3	0.3
Hepa$_{ION}$-TiCaPCON	73.4	6.0	20.3	0	0.4

3.5. Kinetics of antibacterial agent release

UV absorbance spectra of the gentamicin-, 3-carboxyproxyl-, heparin-, and indolicidin-conuganted samples are presented in Figure 6A. The sample with gentamicin sulfate reveals a characteristic maximum at a wavelength of 224 nm, which is in good agreement with available data [39]. Peptide absorbance in the UV spectrum appears as a sum of two peaks in the far- (224 nm) and near-UV (278 nm) regions that can be assigned to the peptide bond and aromatic side chains of tryptophan aromatic amino acid, respectivelly [40]. The UV spectrum of heparin contains two broad maxima at 222 and 256.4 nm. The first peak appears due to the presence of carboxyl groups, while the second one is related to electronic transitions arising from aromatic compounds [44]. The maximum absorption intensitiy of 3-carboxyproxyl is 253 nm, which corresponds to nitroxide bond [45]. Note that DMSO also absorbs in this region, therefore the concentration of released 3-carboxyproxyl can not be determined.

Figure 6B-D shows the resease kinetcis of gentamicin, heparin, and indolicidin from the sample surfaces. The following general regularities can be noted: (i) the released amount of therapeutic agent was higher in the case of electrostatic immobilization, which can be explained either by a larger amount of immibilized compound or its weaker bonding, and (ii) most of the bactericides leached out of the surface within the first 24 h. The electrostatically bonded heparin stopped leaching out after 24. The indolicidin, both electroctatically and covalently immobilized, released for 48 h. The covalently bonded heparin released for as long as 72 h. Interestingly, the gentamicin-grafted samples, especially Gent$_{COV}$-TiCaPCON, demonstrated sustained bactericide release for 120 h: the gentamicin concentration increased from 90 µg/mL (24 h) to 115 µg/mL (120 h).
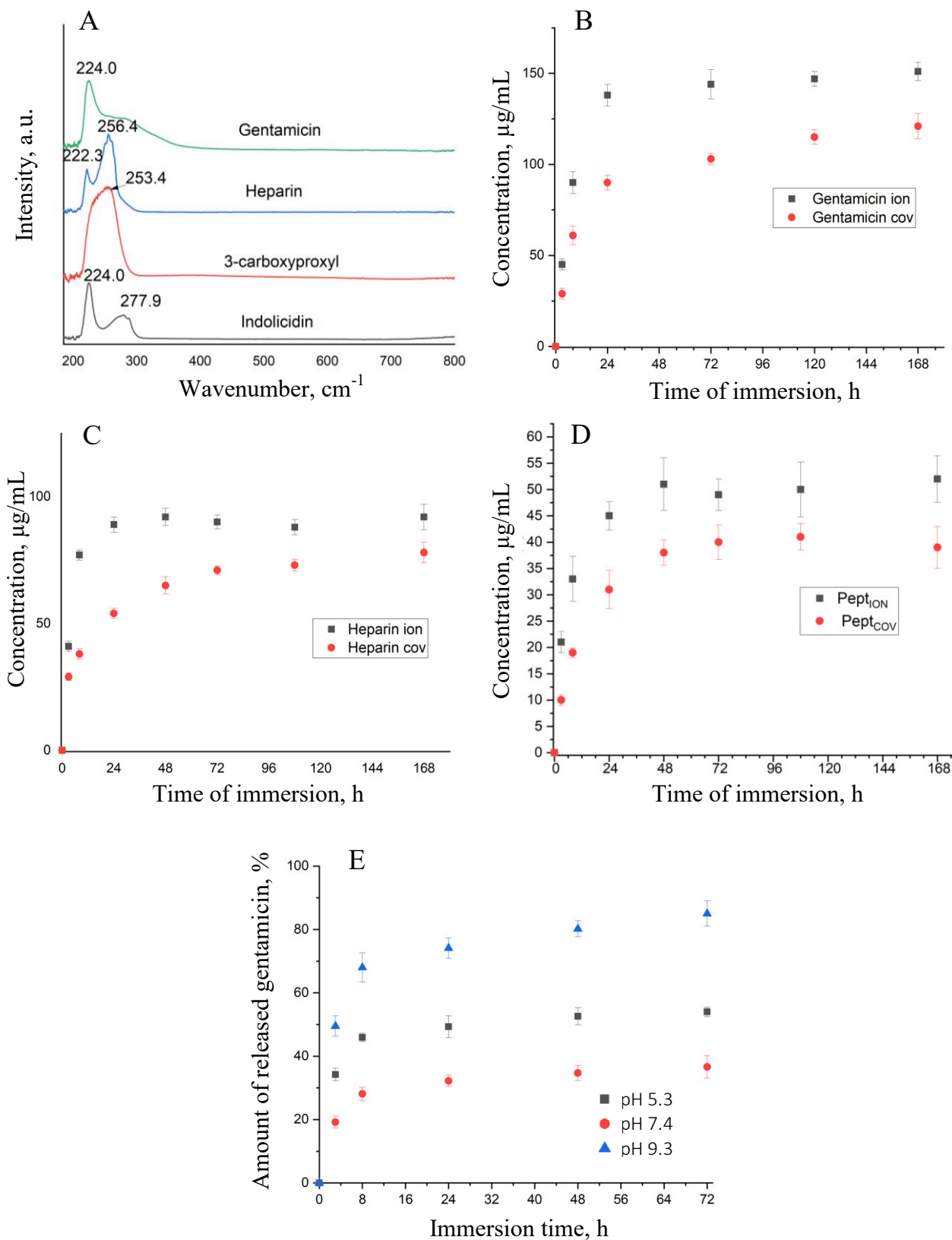
Fig. 6. UV spectra of therapeutic agents (A) and release kinetics of gentamicin (B), heparin (C), and indolicidin (D). pH-sensitive relesae of gentamicin (E).

The pH-sensitive release was studied using the gentamicin-immobilized system (Fig. 6E). The lowest gentamicin release rate was observed at pH 7.4. After 72 h, approximately 37% of immobilized gentamicin was released. This observation is in good agreement with the results of polymer stability tests indicating the highest stability of the COOH polymer in neutral medium (Fig. 2C). In acidic and alkaline environments, accelerated antibiotic release was observed (53% and 83% after 72 h, respectively), which also agrees well with the polymer stability tests. The obtained results indicate that the plasma-deposited polymers with bonded therapeutic agent are pH-sensitive and can respond to a local change in acidity of the environment when bacteria approach.

3.6. Antibacterial activity

Bactericide-bonded COOH-TiCaPCON films were studied toward *E. coli* U20 (antibiotic-sensitive) and K261 (antibiotic-resistant) strains. All samples showed noticeable reduction of *E. coli* U20 strain after 8 h, wherein the covalently bonded gentamicin film exhibited 99.99% bactericidal effect (shown by arrow in Figure 7A). The peptide-bonded samples were not effective toward *E. coli* K261 cells. In contrast, sample NO_{ION} completely inactivated bacterial cells already after 8 h (Figure 6B). Samples $Gent_{ION}$ and $Hepa_{ION}$ eliminated the cells after 24 h, whereas film $Gent_{COV}$ showed 2-log reduction in CFU/mL value.

To estimate the duration of bactericidal effect, some samples were first exposed in NSS for 24 and 48 h. In the case of films NO_{COV} and NO_{ION} that were not subjected to preliminary treatment, no *E. coli* K261 cells were observed already after 8 h (Figure 8A,B). After incubation in NSS for 24 h, the antibacterial effect was less pronounced: the CFU/mL values were found to decrease by about an order of magnitude after 8 h. Film NO_{ION} showed the ability to inhibit the growth of bacterial cells even after exposure in NSS for 48 h as approximately 90% of cells were inactivated by this sample after 8 h. The antibacterial effect of sample NO_{COV} was compared for different initial cell concentrations of *E. coli*, 10^4 and 10^5 CFU/mL (Figure 8A,C). As expected, for the higher initial cell concentration, the bactericidal efficiency of as-fabricated sample was lower (2-log reduction in the CFU/mL value after 24 h) and no antibacterial effect was observed after preliminary exposure in NSS. To assess the ability of bactericide-impregnated samples to prevent biofilm formation, the coupon method was used. The results indicated that only film NO_{COV} completely protected the sample from biofilm build-up (bar 2 in Figure 8e). Sample $Pept_{COV}$ also slowed down the biofilm growth (bar 8 in Figure 8e).
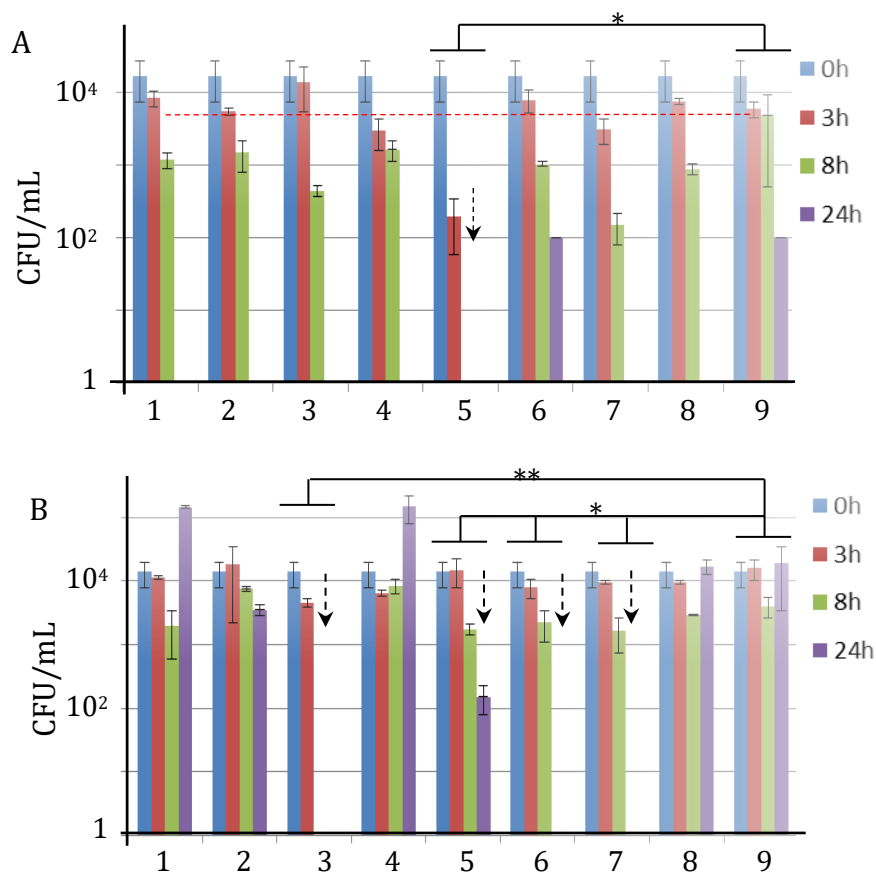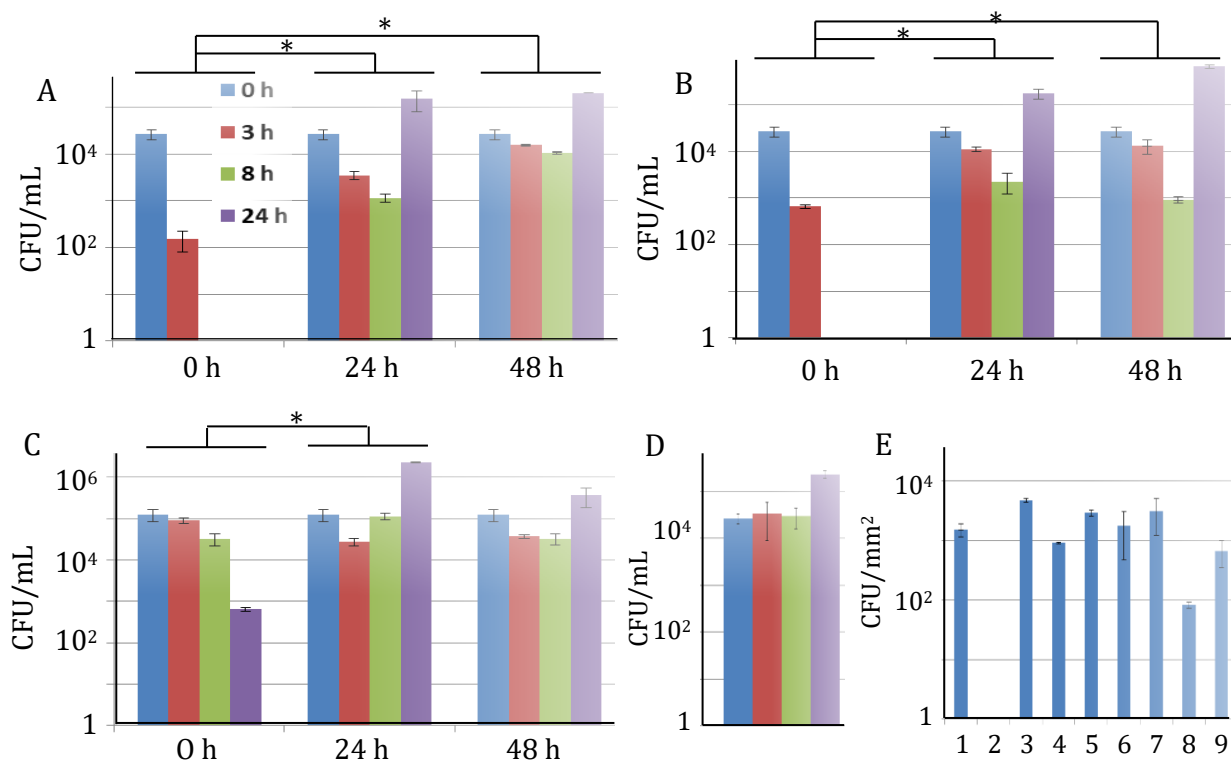
Fig. 7. Antibacterial activity of bactericide-bonded COOH-TiCaPCON samples toward *E. coli* U20 (A) and K261 (B) strains. 1 – Pept$_{ION}$, 2 – Pept$_{COV}$, 3 – NO$_{COV}$, 4 – NO$_{ION}$, 5 – Gent$_{ION}$, 6 – Gent$_{COV}$, 7 – Hepa$_{COV}$, 8 – Hepa$_{ION}$, 9 – Control. Each result is an average of three parallel experiments. All data are presented as mean ± standard deviation. * $p < 0.05$, ** $p < 0.01$.

Additional tests were carried out to assess the antibacterial effect reproducibility. In the case of electrostatically bonded gentamicin, high repeatability of results was observed as all *E. coli* cells were observed to be eliminated after 8 h (Figure 9B). The bactericide efficiency of covalently bonded gentamicin ranged slightly from test to test, varying between 1- or 4-log reductions in the CFU/mL value after 8 h (Figure 9A). The covalently heparin-bonded samples showed >90% cell reduction in all three tests (Figure 9C). When heparin was electrostatically bonded, the results showed a greater spread (from no effect to 99% bactericide effect).

4. Discussion

To sum up, all antibacterial compounds bonded to the surface of COOH-TiCaPCON films were effective against antibiotic-sensitive *E. coli* U20 cells. At an initial concentration of bacterial

cells of 10^4 CFU/mL (which corresponds to the onset of inflammatory process [46]), gentamicin, heparin, and NO-immobilized films had a bactericidal effect toward the antibiotic-resistant *E. coli* K261 strain. The covalently bound nitroxyl radicals not only effectively inhibited the growth of planktonic bacteria, but also prevented biofilm formation. In contrast, the electrostatically bonded NO films showed the highest antibacterial activity (100% after 8 h) and the best reproducibility.

Fig. 8. Antibacterial activity of bactericide-bonded COOH-TiCaPCON samples against *E. coli* K261 strain before (0 h) and after preliminary exposure in NSS for 24 and 48 h: NO_{COV} (A, C), NO_{ION} (B), control (D). Biofilm formation on the sample surfaces (E): 1 – Si, 2 – NO_{COV}, 3 – NO_{ION}, 4 – $Gent_{COV}$, 5 – $Gent_{ION}$, 6 – $Hepa_{COV}$, 7 – $Hepa_{ION}$, 8 – $Pept_{COV}$, 9 – $Pept_{ION}$. Each result is an average of three parallel experiments. All data are presented as mean ± standard deviation. * $p < 0.05$.

We analyzed the effect of pH on the degradation rate of carboxyl groups for primary assessment of the hydrolysis of ether bonds in plasma-deposited polymer. The found results indicated that a change in pH to acidic or alkaline leads to a faster polymer degradation and a higher amount of released gentamicin. The attachment of therapeutic agent occurs through the formation of peptide bonds between the active carboxyl groups of plasma polymer films and amino groups of the antibacterial component. Thus, the release of therapeutic agent can occur as a result of hydrolysis of ether bonds and/or due to degradation of peptide bonds. Note, however, that in a bacterial

environment, the influence of additional factors should be taken into account. For example, in case of gram-negative *E. coli* strain, β-lactam enzymes capable of cleaving amide bonds [47] and esterase, hydrolyzing ether bonds [48], will play an important role in the release of therapeutic agents.
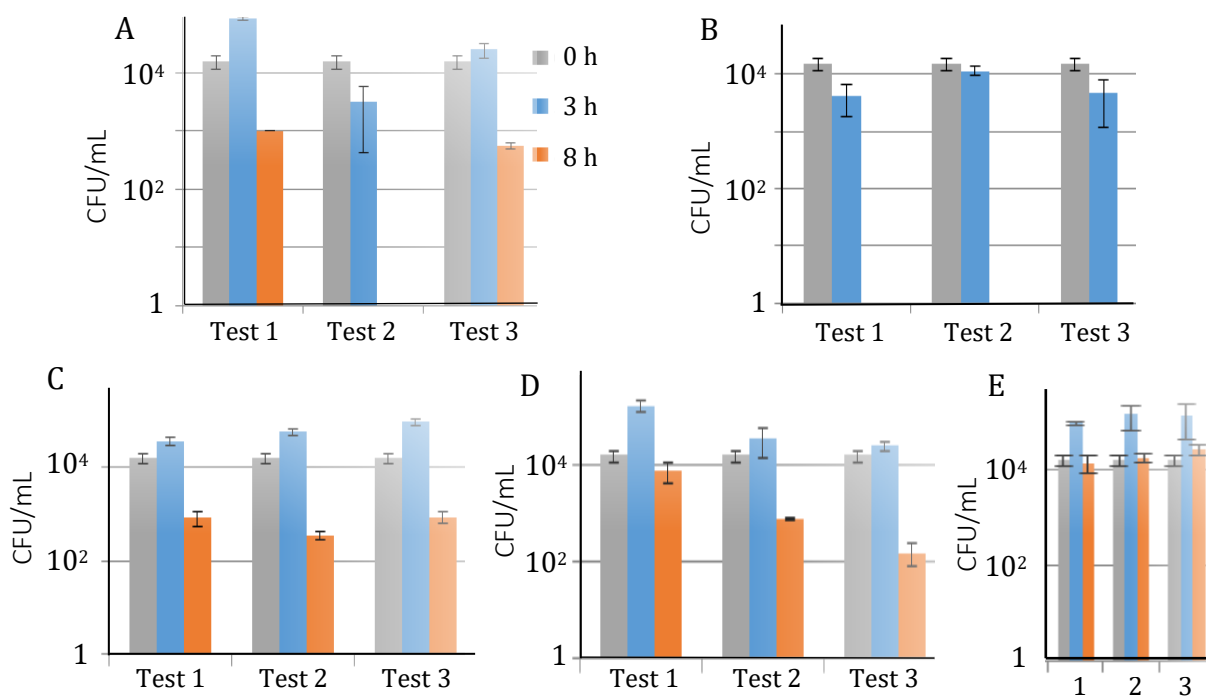
Figure 9. Antibacterial activity of bactericide-bonded COOH-TiCaPCON samples against *E. coli* K261 strain: Gent$_{COV}$ (A), Gent$_{ION}$ (B), Hepa$_{COV}$ (C), Hepa$_{ION}$ (D), control (E). Each result is an average of three parallel experiments. All data are presented as mean ± standard deviation.

There are several factors which can affect antibacterial efficiency from test to test. (i) In the culturing process of clinical isolates of antibiotic-resistant bacteria, the cellular organization of bacteria and their response to bactericidal agents can change. Slowdown in growth of antibiotic-resistant bacteria can be compensated by increased virulence of a pathogen, and the bacteria can easily accumulate compensatory mutations that fully, or partially, restore their original pathogenic abilities [49]. (ii) Insufficient stability and adhesion of a thin plasma polymer film could be another reason. Plasma-produced polymers are known to be highly irregular, randomly cross-linked and branched, and contain trapped radicals [50]. The stability of a C:H:O plasma polymer film in water solution depends on the amount of carbonyl and carboxyl/ester species and decreases at their high amount due to interaction with oxygen [51]. During deposition, the composition of plasma polymer

may have changed due to a slight variation in gas composition (experimental setup was equipped with gas controllers without feedback using optical emission spectroscope).

The main advantage of the strategy proposed in this study is that the therapeutic agent can be attached to the implant surface in a very small dose and act locally in the area of acute inflammation. We clearly demonstrate that using a combination of plasma polymerization and methods of carbodiimide chemistry it is possible to create stable surfaces grafted with different biomolecules. When compared with the ion release-based approach, in which the release of bactericide ions (Ag, Cu, Zn, etc.) is difficult to control due to various factors affecting their leaching (concentration, agglomeration, surface roughness and oxidation) [52], the proposed method is flexible (different types of therapeutic agents can be grafted), low cost, and easily scalable. In addition, since the bactericide immobilization is through the pH-sensitive plasma polymer, the therapeutic agent/polymer nanohybrids can be used as a "smart" platform for controlled bactericide release in response to a change in pH. This requires additional studies.

We examined and compared two strategies of therapeutic agent immobilization to the surface of COOH-coated bioactive TiCaPCON films by electrostatic and covalent interactions. The electrostatic attachment implies that sample is immersed into bactericidal solution. This method is relatively simple and does not require additional chemical reagents. However, fast biocide leaching may lead to a rapid decrease in antibacterial activity [53]. Our results indicated that the released amount of therapeutic agent was higher in case of electrostatic immobilization, which can be explained either by a larger amount of immibilized compound or by its weaker bonding. The electrostatically conjugated bactericides leached out of the surfaces within the first 24 h (Fig. 5B-D).

As an alternative approach, covalent immobilization of biological molecules can be achieved using the methods of carbodiimide chemistry. Energies of ester dissociation [54] and peptide bond formation [55] (in hundreds of kJ/mol range) are significantly higher than those of the ionic bonds which are formed without carbodiimide treatment [56]. Thus, the covalently-bonded gentamicin with the plasma-treated surface is more stable and releases more slowly compared with its ionic immobilization. In this work, COOH-TiCaPCON films with covalently bonded bactericidal agents showed their release for as long as 48 h (indolicidin), 72 (heparin), and 120 h (gentamicin). In the interval between 72 and 120 h, the concentration of gentamicin increased by 13 μg/mL, which is more than reported minimal inhibitory concentration (MIC) for *E. coli* (0.25-0.5 μg/mL [57]). Although in the present work we did not study the long-term antibacterial activity of Gent-COOH-TiCaPCON films, the prolonged biocidal effect (72 h) was shown on Gent-immobilized TiCaPCON films [16]. Covalently immobilized antimicrobial agents (vancomycin and caspofungin) on titanium surface were shown to prevent *Staphylococcus aureus* and *Candida albicans* colonization and

biofilm formation without compromising osseointegration hereby demonstrating the clinical usefulness of such anti-infective surfaces [58]. Possible bactericidal effect of heparin can be attributed to the heparin/ammonia interaction leading to lower ammonia level, which is important for functioning of bacteria [59].

In case of indolicidin, its bactericidal effect was observed against *E. coli* U20 strain only after 24 h. Previous studies indicated that bactericidal efficiency of peptides also correlated with MIC values [60]. Our results can be explained considering two factors: (i) the indilicidin concentration reaches 30 μg/mL after 12 h (Pept$_{ION}$) and 24 h (Pept$_{COV}$), and (ii) the MIC of indolicidin was reported to be in the range of 30-60 μg/mL [61,62]. Apparently, it takes time to start acting peptides on the bacteria.

Orientation of biological molecules on the surface of plasma polymer films is another factor to take into account. For example, change in the orientation of covalently and electrostatically immobilized peptides may affect their interaction with bacteria [60,63]. The indolicidin covalently tethered to polymer surface showed reduced number of adhered *E. coli* cells compared with the Pept$_{ION}$ counterpart (Fig. 8E). This observation is consistent with the earlier studies which demonstrated that covalently immobilized nitroxide prevents growth of *Pseudomonas aeruginosa* biofilm [64].

In the case of covalent immobilization, release of therapeutic agent may last as long as for several months [65], which is not always desirable for toxicity reasons. In our experiments, the polymer layer was quite thin (~20 nm) and therefore the concentration of active functional carboxyl groups that were used for covalent immobilization of therapeutic agents was relatively low. By adjusting the thickness of such a polymer layer (as was shown above, an increase in deposition time from 2 to 20 min leads to an increase in coating thickness from 20 nm to 230 nm), the amount of covalently bonded and released bactericide can be controlled. Importantly, available data indicate that the surface immobilization of a small amount of therapeutic agent does not lead to toxicity as it was recently proved for gentamicin-grafted biodegradable polymer nanofibers [17] and demonstrated for some other gentamicin-, heparin-, 3-carboxy-proxyl- (Table 3), and nitroxide-conjugated materials [63]. Importantly, film NO$_{ION}$ exhibited superior antifouling properties (Fig. 7E). There are only a few works that attempted to use surface tethered nitroxides as antibacterial coatings [66,67]. The anti-biofilm activity of polynitroxides was recently reported against *Pseudomonas aeruginosa* at nitroxide monomer concentrations as low as 30 wt% [66]. Coadministration of nitroxide (covalently linking to the ciprofloxacin moiety) with antibiotic may improve biofilm eradication activity and reduce the MIC of antibiotic [68]. Moreover, nitroxides can exhibit antioxidant effect against H_2O_2-induced radicals and provide radiation protection [69]. The biocidal activity of immobilized AMPs depends on the preservation of their structure: only

peptides retaining their ability to form amphipathic a-helices or the secondary b-sheet structure have antibacterial activity [70]. The covalently attached AMPs may lose their antibacterial characteristics [71]. Moreover, peptides are sensitive to the action by endogenous proteases that limits their clinical application [72].

Table 3

Biocompatibility of surfaces with immobilized therapeutic agents.

Antibacterial agent	Substrate	Type of cells	Type of immobilization	Biocompatibility	Ref.
Gentamicin	Chitosan film	MC3T3-E1	Covalent	Biocompatibility	73
	Sol-gel glass	Rabbit model (*in vivo*)	Physical sorption	Biocompatibility	74
Heparin	Vascular scaffold	EA.hy926 endothelial cells	Covalent	Stimulate cell proliferation No cytotoxicity	75
3-Carboxy-proxyl	Dendrimer	MRC-5	Covalent	No cytotoxicity	76
Indolicidin	Ag nanoparticles	Vero cells	Covalent	Cytotoxicity depends on indolicidin concentration	77

5. Conclusions

1. Four types of therapeutic agents (antibiotic (gentamicin), antimicrobial peptide (indolicidin), anti-adhesive molecules (heparin) and nitroxide radicals (2,2,5,5-tetramethyl-3-carboxyl-pyrrolidine-1-oxyl)) were successfully attached to the surface of nanostructured biocompatible TiCaPCON films through sequential polymerization in COOH-rich plasma and carbodiimide chemistry processing.

2. All types of surface modifications led to the formation of hydrophilic surfaces with water contact angle values in the range of 26-56°.

3. The therapeutic agent-conjugated samples demonstrated a fast bactericide release within the first 24 h. The bactericide concentration was higher in the case of ionic immobilization. The sample with electrostatically bonded heparin completelly leached out after 24 h. The samples with electroctatically and covalently immobilized indolicidin and covalently bonded heparin released for 48 and 72 h, respectivelly, whereas the gentamicin-grafted sample demonstrated sustained bactericide release for 120 h.

4. Change in the acidity of medium from neutral to acidic or alkaline led to a faster COOH polymer degradation and a higher amount of released gentamicin.

5. All antibacterial substances bonded to the surface of COOH-TiCaPCON films were effective against the antibiotic-sensitive *E. coli* U20 cells. At initial bacterial cell concentration of 10^4 CFU/mL, gentamicin, heparin, and NO-immobilized films showed a pronounced antibacterial effect toward the antibiotic-resistant *E. coli* K261 strain. The sample with covalently attached nitroxide radicals not only effectively inhibited the growth of planktonic bacteria, but also prevented biofilm formation. The sample with electrostatically immobilized nitroxide radicals showed the highest antibacterial activity (99.99% after 8 h) and the best reproducibility.

CRediT authorship contribution statement

Elizaveta S. Permyakova: Methodology, Investigation, Writing – original draft. **Philipp V. Kiryukhantsev-Korneev:** Investigation. **Viktor A. Ponomarev:** Investigation. **Alexander N. Sheveyko:** Investigation. **Sergey A. Dobrynin:** Investigation. **Josef Polčak:** Investigation. **Pavel V. Slukin:** Validation. **Sergey G. Ignatov:** Validation. **Anton Manakhov:** Investigation. **Sergei A. Kulinich:** Writing – review & editing. **Dmitry V. Shtansky:** Conceptualization, Supervision, Formal analysis.

Declaration of Competing Interest

The authors declare that they have no known competing financial interests or personal relationships that could have appeared to influence the work reported in this paper.

Acknowledgments

References

[1] C.R. Arciola, D. Campoccia, Implant infections: adhesion, biofilm formation and immune evasion, Nat. Rev. Microbiol. 16 (2018) 397–409.

[2] M. Wang, T. Tang, Surface treatment strategies to combat implant-related infection from the beginning, J. Orthop. Transl. 17 (2019) 42–54.

[3] N. Rabin, Y. Zheng, C. Opoku-Temeng, Y. Du, E. Bonsu, H.O. Sintim, Biofilm formation mechanisms and targets for developing antibiofilm agents, Future Med. Chem. 7 (2015) 493–512.

[4] M. Cloutier, D. Mantovani, F. Rosei, Antibacterial coatings : challenges, perspectives, and opportunities, Trends Biotechnol. 12 (2015) 1–16.

[5] S.H. Nemati, A. Hadjizadeh, Gentamicin-eluting titanium dioxide nanotubes grown on the ultrafine-grained titanium, AAPS PharmSciTech. 18 (2017) 2180-2187.

[6] F. Siedenbiedel, J.C. Tiller, Antimicrobial polymers in solution and on surfaces: overview and functional principles, Polymers (Basel)4 (2012) 46–71.

[7] J.A. Lichter, K.J. Van Vliet, M.F. Rubner, Design of antibacterial surfaces and interfaces: polyelectrolyte multilayers as a multifunctional platform, Macromolecules 42 (2009) 8573–8586.

[8] X. Shi, Y. Ye, H. Wang, F. Liu, Z. Wang, Designing pH-responsive biodegradable polymer coatings for controlled drug release via vapor-based route, ACS Appl. Mater. Interfaces 10 (2018) 38449–38458.

[9] T. Fouquet, H. Ibn, E. Ahrach, C. Becker, T.N.T. Phan, F. Ziarelli, D. Gigmes, D. Ruch, Water sensitive coatings deposited by aerosol assisted atmospheric plasma process: tailoring the hydrolysis rate by the precursor chemistry, Plasma Process. Polym.12 (2015) 1293–1301.

[10] P. Gentile, I. Carmagnola, Modulation of release kinetics by plasma polymerization of ampicillin-loaded β -TCP ceramics, J. Phys. D Appl. Phys. 49 (2016) 304004–304014.

[11] S. Myung, S. Jung, B. Kim, Immobilization and controlled release of drug using plasma polymerized thin film, Thin Solid Films 584 (2015) 13–17.

[12] Z. Yang, J. Wang, R. Luo, M.F. Maitz, F. Jing, H. Sun, N. Huang, The covalent immobilization of heparin to pulsed-plasma polymeric allylamine films on 316L stainless steel and the resulting effects on hemocompatibility, Biomaterials 31 (2010) 2072–2083.

[13] B.R. Coad, M. Jasieniak, S.S. Griesser, H.J. Griesser, Controlled covalent surface immobilization of proteins and peptides using plasma methods, Surf. Coat. Technol. 233 (2013) 169–177.

[14] K. Vasilev, S.S. Griesser, H.J. Griesser, Antibacterial surfaces and coatings produced by plasma techniques, Plasma Process. Polym. 8 (2011) 1010–1023.

[15] J. Liang, J. She, H. He, Zh. Fan, S. Chen, J. Li, B. Liu A new approach to fabricate polyimidazolium salt (PIMS) coatings with efficient antifouling and antibacterial properties, Appl. Surf. Sci. 478 (2019) 770-778.

[16] I.V. Sukhorukova, A.N. Sheveyko, A. Manakhov, I.Y. Zhitnyak, N.A. Gloushankova, E.A. Denisenko, S.Yu. Filippovich, S.G. Ignatov, D.V. Shtansky, Synergistic and long-lasting antibacterial effect of antibiotic-loaded TiCaPCON-Ag films against pathogenic bacteria and fungi, Mater. Sci. Eng. C 90 (2018) 289-299.

[17] E. Permyakova, A. Manakhov, E. Dvořáková, M. Michlíček, J. Polčak, P.V. Slukin, N.K. Fursova, S.G. Ignatov, N.A. Gloushankova, I.Y. Zhitnyak, I.V. Sukhorukova, L. Zajíčková, D.V. Shtansky, Antibacterial biocompatible PCL nanofibers modified by COOH-anhydride plasma polymers and gentamicin immobilization, Mater. Design. 153 (2018) 60-70.

[18] A. Mazumdar, Y. Haddad, V. Milosavljevic, H. Michalkova, R. Guran, S. Bhowmick, A. Moulick, Peptide-carbon quantum dots conjugate, derived from human retinoic acid receptor responder protein 2, against antibiotic-resistant gram positive and gram negative pathogenic bacteria. Nanomaterials 10 (2020) 325-344.

[19] M.H. Cardoso, B.T. Meneguetti, B.O. Costa, D.F. Buccini, K.G.N. Oshiro, S.L.E. Preza, C.M.E. Carvalho, L. Migliolo, O.L. Franco, Non-lytic antibacterial peptides that translocate through bacterial membranes to act on intracellular targets, Int. J. Mol. Sci. 20 (2019) 4877–4900.

[20] A. Onishi, K. St Ange, J.S. Dordick, R.J. Linhardt, Heparin and anticoagulation, Front. Biosci. - Landmark 21 (2016) 1372–1392.

[21] W. Zhou, Z. Jia, P. Xiong, J. Yan, M. Li, Y. Cheng, Y. Zheng, Novel pH-responsive tobramycin-embedded micelles in nanostructured multilayer-coatings of chitosan/heparin with efficient and sustained antibacterial properties, Mater. Sci. Eng. C 90 (2018) 693–705.

[22] D.T. Allimuthu, Role of reactive oxygen species (ROS) in therapeutics and drug resistance in cancer and bacteria, J. Med. Chem. 60 (2017) 1–68.

[23] C. Liao, Y. Li, S.C. Tjong, Visible-light active titanium dioxide nanomaterials with bactericidal properties, Nanomaterials 10 (2020) 124–180.

[24] M.J.R. Ahonen, D.J. Suchyta, H. Zhu, M.H. Schoenfisch, Nitric oxide-releasing alginates, Biomacromolecules 19 (2019) 1189–1197.

[25] L. Yuan, D.L. Slomberg, M.H. Schoenfisch, Nitric oxide-releasing chitosan oligosaccharides as antibacterial agents, Biomaterials 35 (2015) 1716–1724.

[26] H. Jin, L. Yang, M.J.R. Ahonen, M.H. Schoenfisch, Nitric oxide-releasing cyclodextrins, J. Am. Chem. Soc. 140 (2019) 14178–14184.

[27] N. Barraud, M.V. Storey, Z.P. Moore, J.S. Webb, S.A. Rice, S. Kjelleberg, Nitric oxide-mediated dispersal in single- and multi-species biofilms of clinically and industrially relevant microorganisms, Microb. Biotechnol. 2 (2009) 370–378.

[28] N. Liu, Y. Xu, S. Hossain, N. Huang, D. Coursolle, J.A. Gralnick, E.M. Boon, Nitric oxide regulation of cyclic di-GMP synthesis and hydrolysis in shewanella woodyi, Biochemistry 51 (2012) 2087–2099.

[29] P. Krukowski, W. Kozlowski, W. Olejniczak, Z. Klusek, M. Puchalski, P. Dabrowski, P.J. Kowalczyk, K. Gwozdzinski, G. Grabowski Formation of dense nitroxide radical layers on the Au(1 1 1) substratefor ESN-STM measurement, Appl. Surf. Sci. 255 (2008) 1921–1928.

[30] G.I. Likhtenshtein, J. Yamauchi, S. Nakatsuji, A.I. Smirnov, R. Tamura, Biomedical and medical applications of nitroxides, In Nitroxides : Applications in Chemistry, Biomedicine, and Materials Science, Wiley-VCH Verlag GmbH & Co. KGaA, 2008, 371–399.

[31] S.A. Alexander, C. Kyi, C.H. Schiesser, Nitroxides as anti-biofilm compounds for the treatment of pseudomonas aeruginosa and mixed-culture biofilms, Org. Biomol. Chem. 13 (2015) 4751–4759.

[32] A.D. Verderosa, S.C. Mansour, C. de la Fuente-núñez, R.E.W. Hancock, K.E. Fairfull-Smith, Synthesis and evaluation of ciprofloxacin-nitroxide conjugates as anti-biofilm agents, Molecules 21 (2016) 841–857.

[33] A. Manakhov, M. Michlíček, A. Felten, J.-J. Pireaux, D. Nečas, L. Zajíčková, XPS depth profiling of derivatized amine and anhydride plasma polymers: evidence of limitations of the derivatization approach, Appl. Surf. Sci. 394 (2017) 578–585.

[34] D.V. Shtansky, E.A. Levashov, I.V. Batenina, N.A. Gloushankova, N.Y. Anisimova, M.V. Kiselevsky, I.V. Reshetov, Recent progress in the field of multicomponent bioactive nanostructured films, RCS Advances 3 (2013) 11107-11115.

[35] M.J.E. Fischer, Amine coupling through EDC/NHS: a practical approach, Methods Mol. Biol. 627 (2010) 55–73.

[36] G. Sosnovsky, Z. Cai, A Study of the Favorskii rearrangement with 3-Bromo-4-oxo-2,2,6,6-tetramethylpiperidine-1-oxyl, J. Org. Chem. 60 (1995) 3414–3418.

[37] M. Gozdziewska, G. Cichowicz, K. Markowska, K. Zawada, E. Megiel, Nitroxide-coated silver nanoparticles: synthesis, surface physicochemistry and antibacterial activity, RSC Adv. 5 (2015) 58403-58415.

[38] A. Manakhov, P. Kiryukhantsev-Korneev, M. Michlíček, E. Permyakova, E. Dvořáková, J. Polčák, Z. Popov, M. Visotin, D.V. Shtansky, Grafting of carboxyl groups using $CO_2/C_2H_4/Ar$ pulsed plasma: theoretical modeling and XPS derivatization, Appl. Surf. Sci. 435 (2018) 1220–1227.

[39] S. Naveed, N. Waheed, S. Nazeer, F. Qamar, Degradation study of gentamicin by UV spectroscopy, Am. J. Chem. Appl. 1 (2014) 36–39.

[40] M.R. Liyanage, K. Bakshi, D.B. Volkin, C.R. Middaugh, Ultraviolet absorption spectroscopy of peptides, In Therapeutic Peptides: Methods and Protocols, Methods in Molecular Biology; Andrew E. Nixon (ed.), Ed.; Springer 1088 (2014) 225–236.

[41] C. Larimer, E. Winder, R. Jeters, M. Prowant, I. Nettleship, R. S. Addleman, G. T. Bonheyo. A method for rapid quantitative assessment of biofilms with biomolecular staining and image analysis, Anal. Bioanal. Chem. 408 (2009) 999–1008.

[42] V.A. Ponomarev, I.V. Sukhorukova, A.N. Sheveyko, E.S. Permyakova, A.M. Manakhov, S.G. Ignatov, N.A. Gloushankova, I.Y. Zhitnyak, O.I. Lebedev, J. Polčák, A.M. Kozmin, D.V. Shtansky, Antibacterial performance of TiCaPCON films incorporated with Ag, Pt and Zn: bactericidal ions versus surface micro-galvanic interactions, ACS Appl. Mater. Interfaces 10 (2018) 24406-24420.

[43] I.A. Grigor'ev, M.M. Mitasov, G.I. Shchukin, L.B. Volodarskii, Use of Raman spectroscopy to identify nitroxyl group of cyclic nitroxyl radicals, Bull. Acad. Sci. USSR 28 (1979) 2421–2424.

[44] M.A. Lima, T.R. Rudd, E.H.C. de Farias, L.F. Ebner, T.F. Gesteira, L.M. de Souza, A. Mendes, C.R. Cordula, J.R.M. Martins, D. Hoppensteadt, J. Fareed, G.L. Sassaki, E.A. Yates, I.L.S. Terariol, H.B.

Nader, A new approach for heparin standardization: combination of scanning UV spectroscopy, nuclear magnetic resonance and principal component analysis, PLoS One 6 (2011) 15970–15979.

[45]   R. Toba, H. Gotoh, K. Sakakibara, Scavenging and characterization of short-lived radicals using a novel stable nitroxide radical with a characteristic UV−vis absorption spectrum, Org. Lett. 16 (2014) 3868–3871.

[46]   R. Orenstein, E. S. Wong. Urinary tract infections in adults Am. Fam. Physician. 59 (1999) 1225-1234.

[47]   C.L. Tooke, P. Hinchliffe, E.C. Bragginton, C.K. Colenso, V.H.A. Hirvonen, Y. Takebayashi, J. Spencer, β-Lactamases and β-lactamase inhibitors in the 21st century, J. Mol. Biol. 431 (2019) 3472–3500.

[48]   A.K. Antonczak, Z. Simova, E.M. Tippmann, A critical examination of Escherichia coli esterase activity, J. Biol. Chem. 284 (2009) 28795–28800.

[49]   B. R. Levin, V. Perrot, N. Walker, Compensatory mutations, antibiotic resistance and the population genetics of adaptive evolution in bacteria. Genetics 154 (2000) 985-997.

[50]   M. Drabik, D. Lohmann, J. Hanus, A. Shelemin, P. Rupper, H. Biederman, D. Hegemann, Structure and stability of C:H:O plasma polymer films co-polymerized using dimethyl carbonate, Plasma 1 (2018) 156-176.

[51]   M. Vandenbossche, D. Hegemann, Recent approaches to reduce aging phenomena in oxygen- and nitrogen-containing plasma polymer films: An overview. Curr. Opin. Solid State Mater. Sci. 2018, 22, 26–38.

[52]   I.V. Sukhorukova, A.N. Sheveyko, N.V. Shvindina, E.A. Denisenko, S.G. Ignatov, D.V. Shtansky, Approaches for controlled Ag$^+$ ion release: influence of surface topography, roughness, and bactericide content, ACS Appl. Mater. Interfaces 9 (2017) 4259−4271.

[53]   N. Gour, K.X. Ngo, C. Vebert-Nardin, Anti-infectious surfaces achieved by polymer modification. Macromol. Mater. Eng. 299 (2014) 648–668.

[54]   V.E. Tumanov, E.T. Denisov, Estimation of the dissociation energies of O–O, C–O, and O–H bonds in acyl peroxides, acids, and esters from kinetic data on the degradation of diacyl peroxides, Petr. Chem. 45 (2005) 237-248.

[55]   F. Tureček, N-Cα bond dissociation energies and kinetics in amide and peptide radicals. Is the dissociation a non-ergodic process? J. Am. Chem. Soc.125 (2003) 5954–5963.

[56]   L. Largo, P. Redondo, V.M. Rayón, A. Largo, C. Barrientos, The reaction between NH$_3^+$ and CH$_3$COOH: a possible process for the formation of glycine precursors in the interstellar medium, Astronom. Astrophys. 516 (2010) A79.

[57]   J.M. Andrews, Determination of minimum inhibitory concentrations, J. Antimicrob. Chem. S1 (2001) 5-16.

[58]   S. Kucharíkova´, E. Gerits, K. De Brucker, A. Braem, K. Ceh, G. Majdič, T. Španič, E. Pogorevc, N. Verstraeten, H. Tournu, N. Delattin, F. Impellizzeri, M. Erdtmann, A. Krona, M. Lövenklev, M. Knezevic, M. Fröhlich, J. Vleugels, M. Fauvart, W.J. de Silva, K. Vandamme, J. Garcia-Forgas,

B.P.A. Cammue, J. Michiels, P. Van Dijck. K. Thevissen, Covalent immobilization of antimicrobial agents on titanium prevents Staphylococcus aureus and Candida albicans colonization and biofilm formation, J. Antimicrob. Chemother. 71 (2016) 936–945.

[59] J.D. Simen, M. Löffler, G. Jäger, K. Schäferhoff, A. Freund, J. Matthes, J. Müller, R. Takors, Transcriptional response of Escherichia coli to ammonia and glucose fluctuations, Microb. Biotechnol. 10 (2017) 858–872.

[60] J. Hernandez-Montelongo, Y.R. Corrales Ureña, D. Machado, M. Lancelloti, M.P. Pinheiro, K. Rischka, P.N. Lisboa-Filho, M.A. Cotta, Electrostatic immobilization of antimicrobial peptides on polyethylenimine and their antibacterial effect against *Staphylococcus epidermidis*, Coll. Surf. B 164 (2018) 370-378.

[61] A. Ebbensgaard, H. Mordhorst, M.T. Overgaard, C.G. Nielsen, F.M. Aarestrup, E.B. Hansen, Comparative evaluation of the antimicrobial activity of different antimicrobial peptides against a range of pathogenic bacteria, PLoS One 10 (2015) e0144611.

[62] C. Zannella, S. Shinde, M. Vitiello, A. Falanga, E. Galdiero, A. Fahmi, B. Santella, L. Nucci, R. Gasparro, M. Galdiero, M. Boccellino, G. Franci, M. Di Domenico, Antibacterial activity of indolicidin-coated silver nanoparticles in oral disease, Appl. Sci. 10 (2020) 1837.

[63] K.B. Alici, I.F. Gallardo, Detecting secondary structure and surface orientation of helical peptide monolayers from resonant hybridization signals, Sci. Reports 3 (2013) 2956.

[64] H. Woehlik, M. Trimble, S.C. Mansour, D. Pletzer, V. Trouillet, A. Welle, L. Barner, R.E.W. Hancock, C. Barner-Kowollik, K.E. Fairfull-Smith, Controlling biofilm formation with nitroxide functional surfaces, Polymer Chem. 10 (2019) 4252-4258.

[65] C. Pan, Z. Zhou, X. Yu, Coatings as the useful drug delivery system for the prevention of implant-related infections, J. Orthop. Surg. Res. 13 (2018) 220-231.

[66] N.R.B. Boase, M.D.T. Torres, N.L. Fletcher, C. de la Fuente-Nunez, K.E. Fairfull-Smith, Polynitroxide copolymers to reduce biofilm fouling on surfaces, Polymer Chem. 9 (2018) 5308-5318.

[67] M. Gozdziewska , G. Cichowicz , K. Markowska , K. Zawada and E. Megiel , Nitroxide-coated silver nanoparticles: synthesis, surface physicochemistry and antibacterial activity, RSC Adv. 5 (2015) 58403-58415.

[68] A.D. Verderosa, R. Dhouib, K.E. Fairfull-Smith, M. Totsika, Nitroxide functionalized antibiotics are promising eradication agents against Staphylococcus aureus siofilms, Antimocrob. Agents Chemotherapy 64 (2020) e01685-19.

[69] B.P. Soule, F. Hyodo, K. Matsumoto, N.L. Simone, J.A. Cook, M.C. Krishna, J.B. Mitchell, The chemistry and biology of nitroxide compounds, Free Radic. Biol. Med. 42 (2007) 1632–1650.

[70] W.M. Cho, B.P. Joshi, H. Cho, K.H. Lee, Design and synthesis of novel antibacterial peptide–resin conjugates, Bioorg. Med. Chem. Lett. 17 (2007) 5772–5776.

[71] F. Costa, I.F. Carvalho, R.C. Montelaro, P.M. Gomes, C.L. Martins, Covalent immobilization of antimicrobial peptides (Amps) onto biomaterial surfaces, Acta Biomat. 7 (2011) 1431–1440.

[72] H.M. Werner, C.C. Cabalteja, W.S. Horne, Peptide backbone composition and protease susceptibility: impact of modification type, position, and tandem substitution, Chembiochem. 17 (2016) 712–718.

[73] Y. Liu, P. Ji, H. Lv, Y. Qin, L. Deng, Gentamicin modified chitosan film with improved antibacterial property and cell biocompatibility, Int. J. Biol. Macromolecules 98 (2017) 550–556.

[74] L. Meseguer-Olmo, M.J. Ros-Nicolás, M. Clavel-Sainz, V. Vicente-Ortega, M. Alcaraz-Baños, A. Lax-Pérez, D. Arcos, C.V. Ragel, M. Vallet-Regí, Biocompatibility and in vivo gentamicin release from bioactive sol-gel glass implants, J. Biomed. Mater. Res. 61 (2002) 458-465.

[75] Y. Tao, T. Hu, Z. Wu, H. Tang, Y. Hu, Q. Tan, C. Wu, Heparin nanomodification improves biocompatibility and biomechanical stability of decellularized vascular scaffolds, Int. J. Nanomedicine 7 (2012) 5847-5858.

[76] L.F. Pinto, V. Lloveras, S. Zhang, F. Liko, J. Veciana, J. Munoz-Gomez, J. Vidal-Gancedo, Fully water-soluble polyphosphorhydrazone-based radical dendrimers functionalized with Tyr-PROXYL radicals as metal-free MRI T1 contrast agents, ACS Appl. Bio Mater. 3 (2020) 369−376.

[77] C. Zannella, S. Shinde, M. Vitiello, A. Falanga, E. Galdiero, A. Fahmi, B. Santella, L. Nucci, R. Gasparro, M. Galdiero, M. Boccellino, G. Franci, M. Di Domenico, Antibacterial activity of indolicidin-coated silver nanoparticles in oral disease, Appl. Sci. 10 (2020) 1837-1850.